Science Translational Medicine
AAAS

Supplementary Materials for

Principles of gait encoding in the subthalamic nucleus of people with Parkinson's disease

Yohann Thenaisie *et al.*

Corresponding author: Eduardo Martin Moraud, eduardo.martin-moraud@chuv.ch

Sci. Transl. Med. **14**, eabo1800 (2022)
DOI: 10.1126/scitranslmed.abo1800

The PDF file includes:

Other Supplementary Material for this manuscript includes the following:

SUPPLEMENTARY MATERIALS AND METHODS

DBS electrode localization

Lead localization was computed using the processing pipeline (26) in the Lead-DBS Matlab toolbox (64) using as inputs pre-operative T1 and T2-weighted magnetic resonance imaging (MRI) scans and a post-operative computed tomography (CT) scan. Briefly, post-operative CT scan was linearly co-registered to pre-operative MRI using advanced normalization tools (ANTs) (65). Co-registrations were visually verified and manually corrected if needed. A brain shift correction step was applied, as implemented in Lead-DBS. All preoperative volumes were used to estimate a precise multi-spectral normalization to ICBM 2009b NLIN asymmetric space (66) applying the ANTs SyN Diffeomorphic Mapping (67) using the preset “effective: low variance default + subcortical refinement”. DBS contacts were automatically pre-reconstructed using the phantom-validated and fully automated PaCER method (68). They were all individually verified.

Joint-specific motor tasks in the neurorobotic platform

Patients were comfortably sitting on an instrumented isokinetic chair (HUMAC NORM, CSMI, USA). The shin of their most affected leg (most affected hemibody, as defined clinically by a neurologist) was strapped to a pushing lever, connected to a dynamometer that measures rotation angles, speeds, and forces applied during a range of experimental conditions (isotonic or isometric exercises, active or passive movements). A screen provided patients with real-time visual feedback about their performance during each task.

Active isotonic movements: Patients were asked to perform a knee extension movement from a resting position (baseline, 90-degree angle of the knee joint) to a full leg extension, and to release the leg back to baseline. 30 repetitions were recorded, interleaved with pauses of 5s duration.

Passive movements: Patients were asked to completely relax their leg (at the baseline position) and to not exert any resistance. The neurorobotic platform was programmed to passively move the patients’ leg with an angular range and speed matching the ones recorded during active isotonic movements. These parameters were kept constant for all trials for each participant. Each trial was interleaved by 5s resting periods.

Isometric transient effort exercises: Patients were asked to push against the lever and to exert a predefined isometric force (either a low or a high force, defined as 33% and 66% of their maximal voluntary contraction respectively, measured as the maximal force each participant could generate and over a 3 second window). Throughout each trial, they received visual feedback of the force being exerted, along with the target. They were asked to release the effort immediately as soon as they reached the target (displayed on the screen as a yellow circle with predefined diameter, it disappeared from the screen as soon as patients reached it).

Isometric sustained effort exercises: Similar to the previous task, but patients were asked to reach and maintain a low or a high force for five seconds before releasing their effort. The target remained displayed on the screen for the duration of the task and patients were instructed to maintain their force within the circle.

Locomotor tasks

Walking tasks (small and big steps): Patients were instructed to stand for about 3 seconds before initiating a sustained bout of walking at their comfortable speed (in a straight line, distance ~7m for externalized patients and ~15m for Percept patients), placing their feet on marked lines on the floor. Marked lines were spaced either 47cm (small) or 70cm (big) apart from each other. When arriving at the end of the bout, patients were instructed to stop and stand for another 3 seconds, before doing a U-turn and starting again.

Obstacle task: Patients were asked to walk at their natural speed in a straight line (without any marks on the floor). An obstacle (height 10.5 cm, length 39.5 cm) was placed on their path. They were requested to stride over it and continue walking normally until the end of the bout.

Biomechanical recordings during gait

Kinematics: Externalized patients were recorded using a whole-body suit endowed with 19 motion sensors on key landmark joints of the legs, arms, trunk and head (Rokoko, Denmark). The suit transmitted accelerometer and magnetometer data wirelessly (100Hz) to a dedicated computer running the Rokoko Studio software, which reconstructed 3D body positions using an inverse-kinematics model. The model was personalized for each patient (definition of body height and segment lengths) on the first day of experiments. Prior to every recording, the initial pose of the model was calibrated during a baseline "standing" position to maximize the accuracy of subsequent movements. Patients implanted with the Percept PC were recorded in a gait lab using an optoelectronic motion capture system (Vicon, UK) that measured 3D positions of key body joints.

Kinematic data was complemented with bilateral triaxial inertial measurement unit (IMU) sensors (Delsys, MA, USA) attached to the patients' shoes, which recorded raw gyroscope signals from the right and left feet (sampling frequency: 148Hz). All recordings were synchronized using dedicated trigger signals.

Electromyographic signals: EMG signals were recorded using a wireless system operating at 1.5kHz (Noraxon, USA). Sensors were placed bilaterally according to SENIAM guidelines (Surface Electro-MyoGraphy for the Non-Invasive Assessment of Muscles, www.seniam.org) on agonist and antagonist muscles of the ankle joint (TA Tibialis Anterior, MG Medial Gastrocnemius, LG Lateral Gastrocnemius) knee joint (VM Vastus Medialis, ST Semitendinosus) and hip joint (RF Rectus Femoris). EMG sensors were covered using protective tape (tegaderm) to prevent them from moving during walking, and to reduce friction with the suit. For patients implanted with a Percept PC stimulator, an additional EMG sensor was placed on the chest for synchronization purposes.

Identification of gait events and definition of locomotor states

Bilateral gait events: We computed periods of walking and turning, along with toe-off and heel-strike events, automatically from gyroscope signals from the right and left feet using a modified version of the two-step framed threshold algorithm[24]. All identified events were validated manually. Briefly:

First, uninterrupted walking sequences were identified from low-pass filtered signals in the sagittal plane (3Hz, 5^{th}-order Butterworth). Mid-swing peaks were detected using a threshold (defined as the average of the top ten peaks and scaled by 0.2. A minimum value of 40 degrees/seconds was taken) and pooled together when less than 3 seconds apart. Peaks of right and left sensors that did not occur consecutively were discarded. Identified walking sequences lasting less than 5 seconds and occurring during concomitant peaks in the coronal plane (which corresponded to turning periods, see below) were also removed.

Within each walking sequence, we extracted heel strike and toe off events. Gyroscope signals were low-pass filtered at 5Hz (5^{th}-order Butterworth). We first refined the identification of mid-swing points. These points needed to be at least 0.5 seconds apart, and greater than a sequence-specific threshold (defined as the mean of all points exceeding the sequence mean). Any mid-swing points not complying with these rules were discarded. We then computed "full contact" times, i.e. when feet were in full contact with the floor (these corresponded to a plateau in the acceleration profiles). They were identified as the maximum of the plateau between consecutive mid-swing peaks. From there, (i) heel strike events were identified as the minima occurring between mid-swing and "full contact" points, and (ii) toe-off events were defined as the minima occurring between "full contact" points and the next mid-swing points.

We then identified turning sequences. The low-pass filtered gyroscope signals in the coronal plane (5Hz, 5^{th}-order Butterworth filter). Turning peaks needed to be superior to a threshold (defined as the

75% percentile of the datapoints exceeding the mean of the whole recording) and at least 0.2 seconds apart. Turning sequences were pooled together: Peaks separated by less than 1.75x the mean inter-peak distance throughout the recording were assumed to belong to the same turning sequence.

Locomotor states: Using the aforementioned gait events, we categorized each time-point of the recordings into five discrete locomotor states, labeled as “standing”, gait “initiation” and “termination”, “continuous walking”, and “turning”.

For each walking sequence, gait initiation was defined as starting 0.5s prior to the first heel-off (time needed for the postural adjustment and bodyweight shift required to lift the leg) until the first heel strike. Gait termination was defined as the last 2 gait cycles (one full step with one leg, and a last one to bring the trailing leg next to the leading leg). Continuous walking corresponded to all steps in between. Standing was defined as the periods between the end of turning and the beginning of gait initiation (standing pre-walk), or as the period between gait termination and the beginning of turning (standing post-walk). This state-machine description of gait was further used for developing gait-state decoders and compute state-related analyses of power.

Computation of muscle synergies

We first computed EMG envelopes for each individual muscle. Raw EMG signals were band-pass filtered (20-500Hz, zero-lag 4^{th}-order Butterworth filter), full-wave rectified and smoothed (zero-lag 4^{th}-order low-pass Butterworth filter at 7 Hz). Envelopes were normalized so that their maximum would be one (each envelope divided by its maximum value throughout the session).

Synergies were derived from all muscle envelopes of the left and right leg together (N = 12 muscles), using recordings from both the small and big stepping tasks. A non-negative matrix factorization (NNMF) algorithm was iteratively run (1000 iterations beginning from 10 initial seed values, randomly selected using the multiplicative update algorithm). For each patient, the 4 first dimensions were kept, and we verified their percentage of variance explained (~90% across patients). We then labeled each one of the extracted synergies as right or left “weight acceptance” or “propulsion” based on the muscle weights and their temporal activations profile. If a muscle exhibited important movement-related artifacts that could not be filtered out, the muscle was removed, and computations performed without it. Despite differences in the muscles that had to be removed across patients, the computed synergies consistently emphasized the “weight acceptance” and “propulsion” phases as most relevant in our task.

To obtain average synergy activation profiles for each task, synergy traces were linearly time interpolated over the 4 phases of each individual gait cycle (stance, swing, and double stance for each leg, as defined by gait events). Gait initiation and termination steps were excluded from this average. The area under the curve of for synergy was computed using trapezoidal numerical integration and compared between tasks across subjects. The synergy sub-space identified on small and big steps was then also used to extract the temporal activation profiles of synergies for other tasks (e.g., mixed steps) by multiplying muscle envelope signals with the identified weights.

Identification of artifacted LFP channels during gait

Gait-related artifacts affect signals predominantly in the low frequencies but can also spread to higher frequencies, which makes them difficult to be removed through standard filtering. Cleaning methods using ICA or advanced signal processing tools have been reported in literature (67) but results and interpretations have remained controversial (68). Moreover, the identification of corrupted channels itself can be tricky, as movement-related neural modulations and artifacts are both locked to the rhythm of gait.

Rather than aiming to identify artifacts in the time-domain, we reasoned that corrupted channels would exhibit important differences in the aperiodic (1/f) component of the power densities (PSD) between rest and walking. The aperiodic component captures the overall baseline power across the spectrum and should not change importantly over consecutive trials (task-related modulations are expected to be captured in the activity of periodic frequency bands).

For each patient, we thus applied the fitting algorithm[24] to the PSD of two separate recordings, one at rest (sitting) and one during walking (from the same session). We then compared their aperiodic (1/f) component: We computed the root mean square error (RMSE) in the range 10 to 90 Hz (region of interest) and ensured that walking did not induce an increase in 1/f power bigger than 50% compared to that sitting (difference of 1.76 dB) (Fig. S10). All channels that exceeded that value were considered as corrupted in the region of interest and discarded for further analyses or decoding purposes. Visual inspection of the spectrogram for channels labeled as "artifacted" consistently showed important low frequency spikes that periodically corrupted the spectrogram and spread to higher frequencies. All retained channels were also verified by visual inspection of their spectrogram.

We note that this approach is highly restrictive, in that channels may still convey useful information (for instance in high frequencies that have a priori not been corrupted) but are nonetheless completely discarded. Overall, N=6 participants exhibited at least one corrupted channel. One patient (implanted with the Percept PC) had to be completely excluded as all contacts (one per hemisphere) were artifacted.

Definition of time-periods of freezing of gait

Clinical evaluation: Periods of freezing of gait were identified based on video analysis by a neurologist expert in movement disorders (A.Z).

Kinematic detection of feet "glued to the ground": Within the periods identified by the neurologist, we computed the times in which the feet of patients were "glued to the ground" using inertial sensors attached to the shoes of the participants. We applied a threshold (1.5x the mean) to the norm of the 7 Hz low-pass filtered accelerometer data of each foot. This defined a binary vector (1 when a foot is moving, 0 when it's static). We added right and left vectors and only preserved states equal to 0 (no movement from either feet) lasting more than 0.5s.

Computation of PSD and band-power during freezing episodes: For each state (stand, walk or freezing), we concatenated all occurrences and computed the overall PSD using Welch method (sliding window of 1s with 50% overlap).

Deep neural network algorithm for the prediction of continuous levels of muscle activation.

Architecture of the convolutional neural network (CNN): Bilateral LFP were used to compute a spectrogram for each contact pair (multitaper). For externalized patients, raw signals were low-passed at 1 kHz and downsampled from 8 kHz to 2 kHz. For Percept PC patients, signals were preprocessed with a hardware bandpass filter in the range of 0.5-100 Hz and sampled at 250 Hz. At each time point (every 10 ms), a spectrogram vector was estimated from a sliding window of 500 ms. 100 consecutive spectrogram vectors were concatenated and fed into the CNN as an input sample with the mapping muscle activation value as the target output.

The CNN was composed of 3 consecutive one-dimensional temporal convolutional layers with increasing receptive fields (layer1: 34 filters with receptive field of view (FoV) of 30 ms, layer 2: 64 filters of 60 ms FoV, layer 3: 128 filters of 120 ms FoV). Each layer was trained to identify the spectro-temporal features that best predict the output at their specific resolution, which were passed to an average-pooling layer with a temporal stride of 2. The output values from the final pooling layer were then flattened and fed into a fully connected layer of 512 nodes, which are finally fed into a single output node without activation function that is mapped to the normalized muscle activation value. Training and testing of the deep neural network were performed using leave-one-trial-out cross-validation on all short and long walking sequences combined. Cross validation was performed at the trial level, i.e. samples were grouped by each trial so that samples from the same trial do not split into training and testing folds, to avoid having optimistic performance due to the temporal proximity of samples.

Performance (Fig. 7 and Fig. S14) was quantified in terms of (i) the capacity to predict changes in synergy amplitude, quantified as the 95% quantile of each walking sequence, and (ii) the timing of synergy modulations, computed as the cross-correlation between the target and modeled traces of each walking sequence.

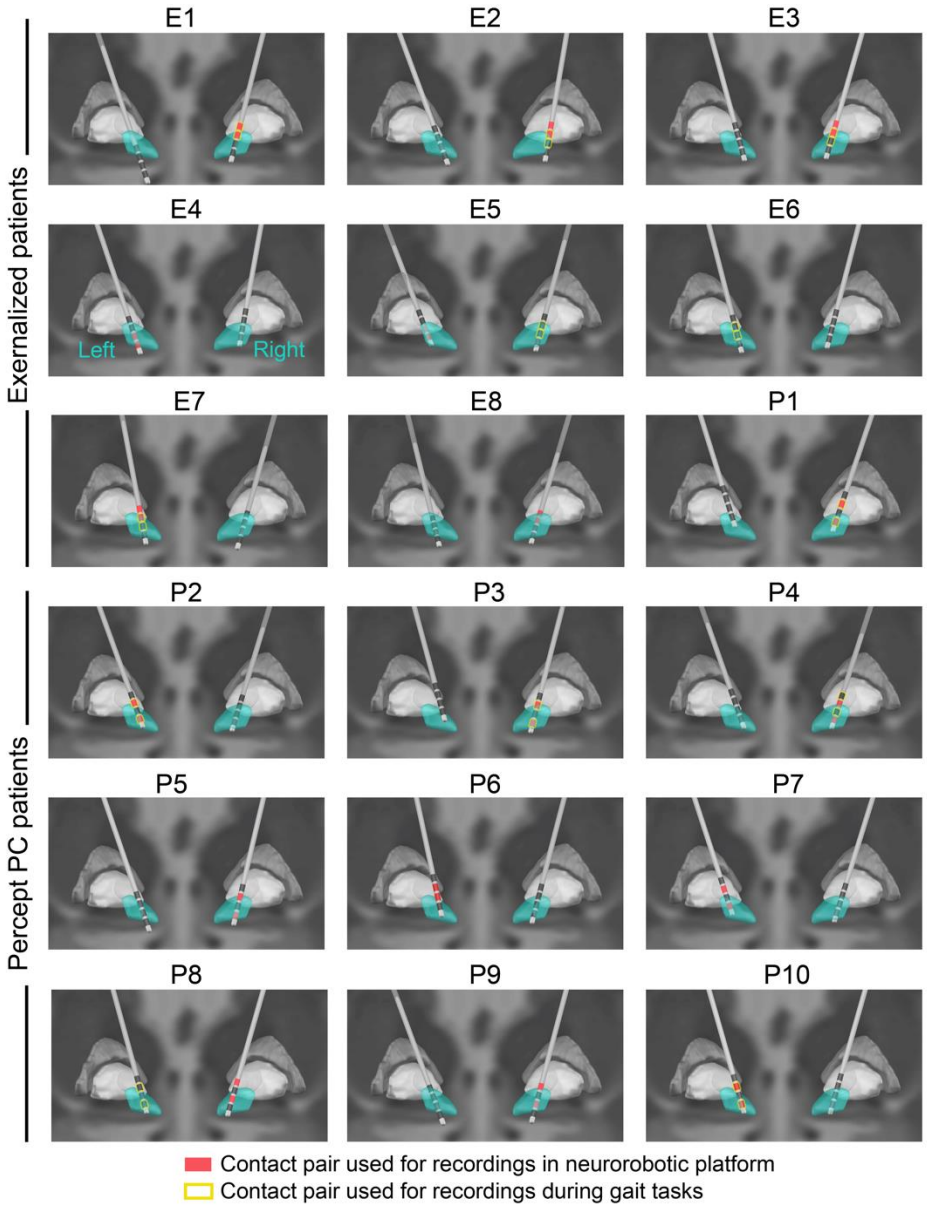

Fig. S1. Anatomical reconstructions of deep brain stimulation lead placement across patients. Recordings were systematically obtained from the most affected STN. Electrode pairs were kept identical for experiments in the neurorobotic platform and during gait, except for patients who exhibited strong gait-related artefacts in those channels: for externalized patients (three contacts per hemisphere), a nearby contact was chosen in such cases. For Percept PC patients (one contact per hemisphere), the other side was considered.

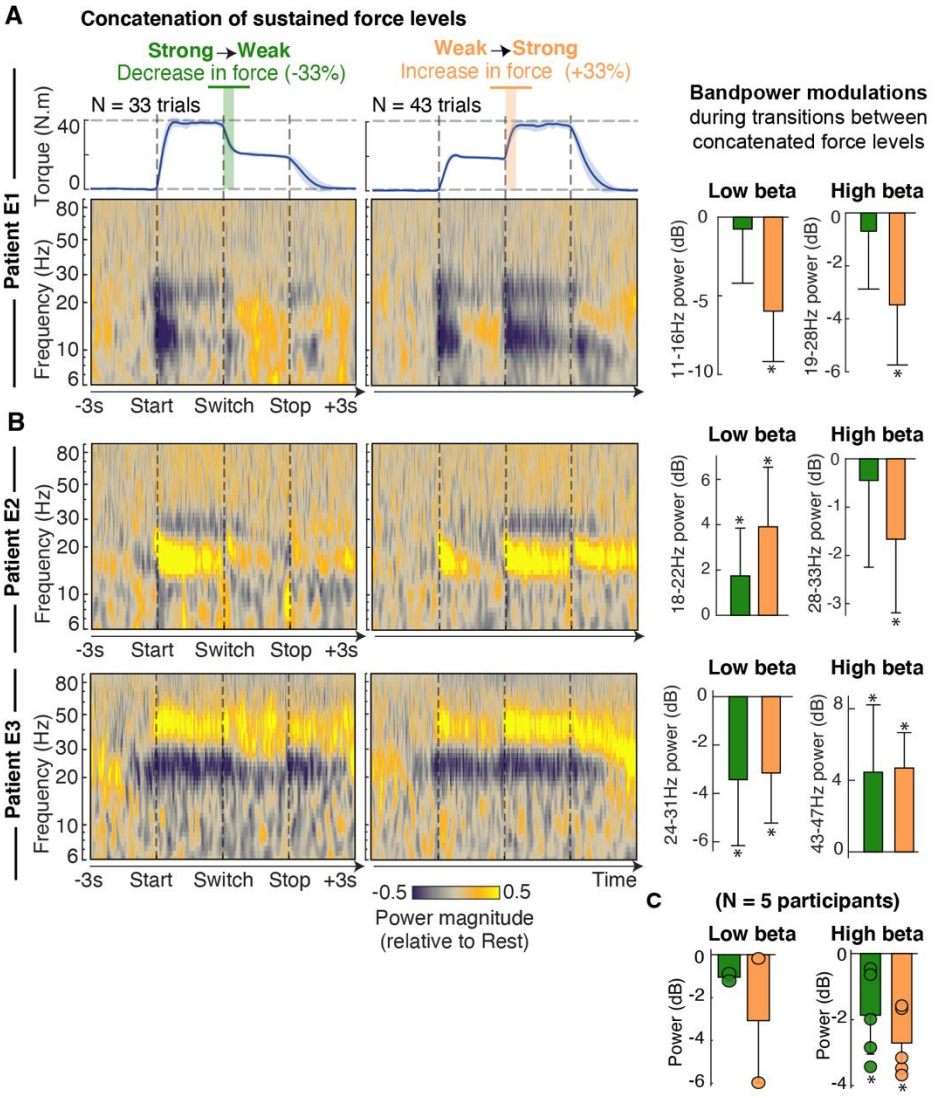

Fig. S2. STN LFP modulations during concatenation of different force intensities. (A) STN modulations during transitions between two different degrees of sustained force, either from a weak to a strong force (left), or inversely (right). Average torque (mean ±SEM) and average spectrograms (rest-normalized, Patient E1). Low and high beta de-synchronizations emerge at the initiation and the termination of muscle activation, as well as during the transitions between force intensities. Barplots display band-power changes (mean ±SD) during transitions compared to baseline. Asterisks display significant differences with respect to baseline (t-test). (B) Similar representations for two other patients exhibiting different frequency band definitions and behaviors: Patient E2 exhibited an increase in 20 Hz power with movement, which scaled up with force. Patient E3 exhibited an increase in low-gamma power that modulated with force. (C) Low and high beta band-power (mean ±SD) across all patients who performed this task (N = 5). Despite clear patient-specific bands and behaviors, the encoding of transitions, states and vigor is present for all subjects in this well-controlled task.

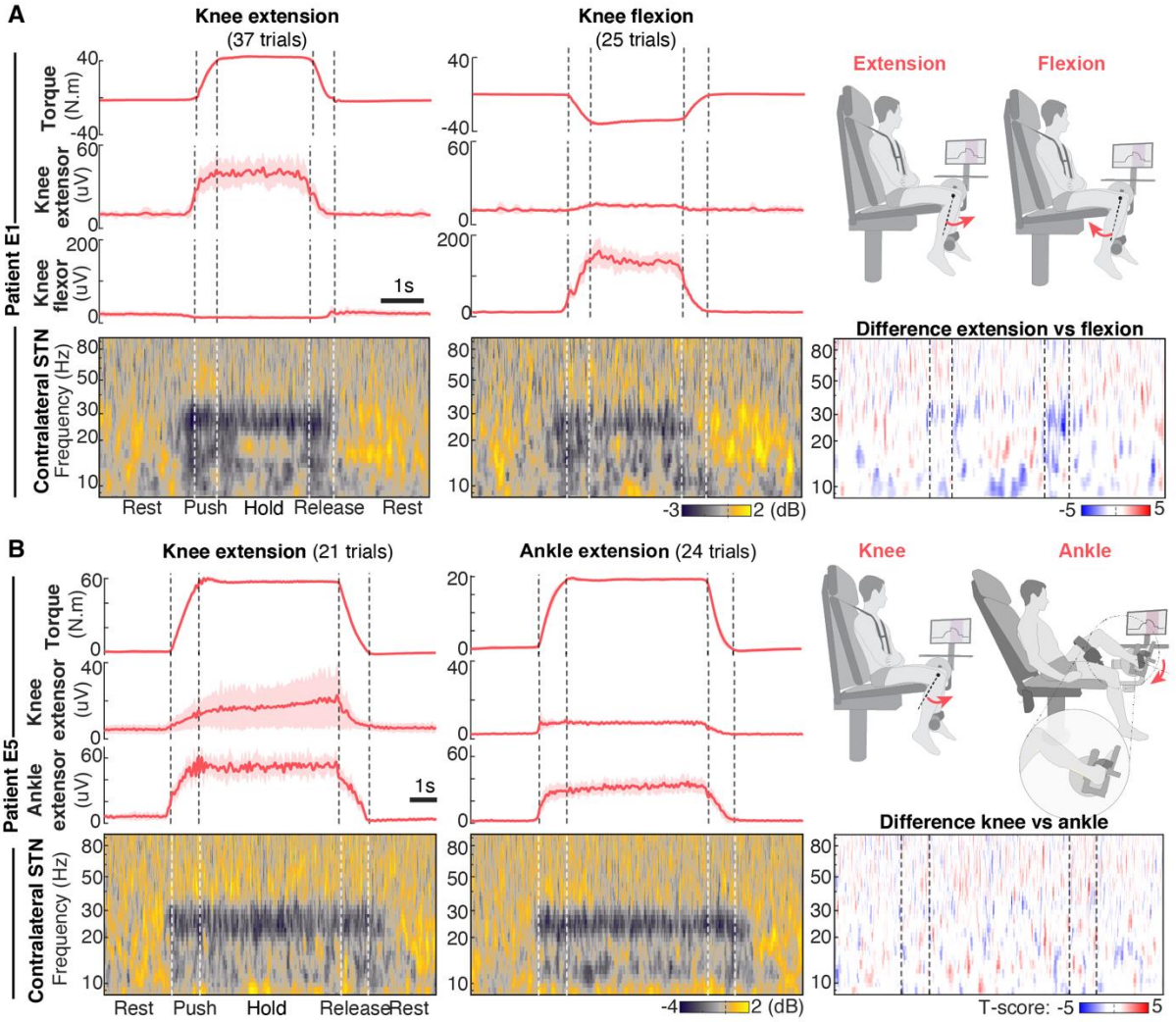

Fig. S3. STN LFP modulations are irrespective of leg joint or movement direction. (A) Patient E1 performed an isometric leg motor task restricted to the knee joint, either in extension or flexion, with two degrees of force intensity (low force 33% and high force 66% of maximal force in each direction). Profiles of torque (mean +/-SD), knee extensor muscle envelope (vastus lateralis) and flexor muscle envelope (semitendinosus), and scalograms of the contralateral STN (most affected hemisphere) normalized to pre-movement. Significance map (t-scores) of the difference between extension versus flexion scalograms (Monte-Carlo cluster randomization) identified no significant clusters in STN modulation despite the difference in movement direction. (B) Patient E5 performed an isometric leg motor task restricted to either the knee or the ankle joint, with two degrees of force. Profiles of torque (mean +/-SD), knee extensor muscle envelope (medial gastrocnemius) or ankle extensor muscle envelope (rectus femoris RF) and scalograms left STN, normalized to pre- movement. Significance map (t-scores) of the difference between knee and ankle scalograms.

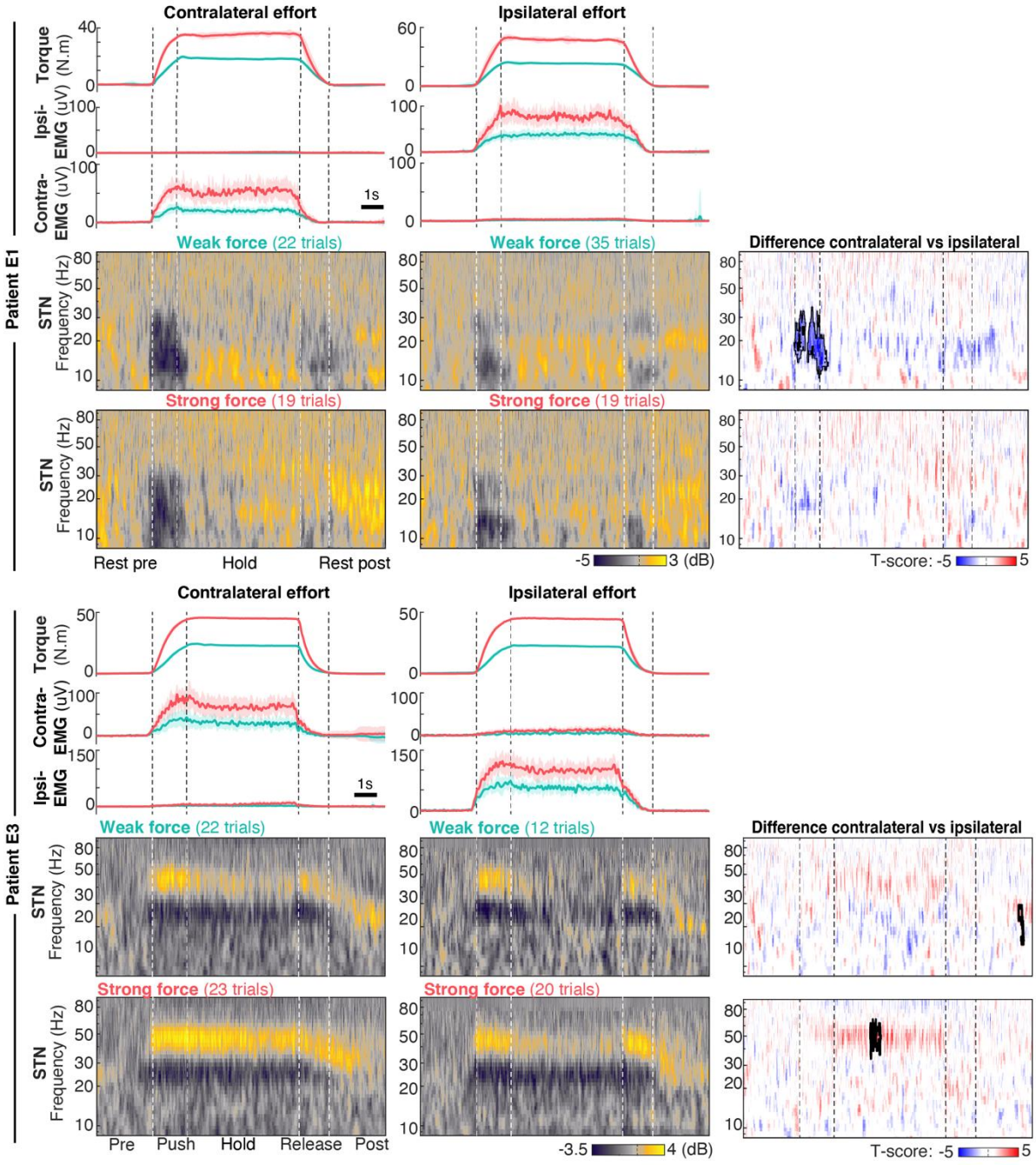

Fig. S4. STN LFP modulations are irrespective of ipsilateral or contralateral leg muscle activation. Two patients (E1, E3) performed an isometric knee extension task with each leg and with two degrees of force intensity. Weak and strong forces were defined as 33% and 66% of the maximal voluntary contraction of each leg, respectively. Temporal profiles of torque (mean +/-SD), knee extensor muscle envelopes and scalograms of the most affected STN. Map of statistical difference (t-map) between contralateral versus ipsilateral movements revealed statistically different clusters, either in beta desynchronization (patient E1) or in low-gamma synchronization (patient E3), which were more pronounced during contralateral than during ipsilateral activations.

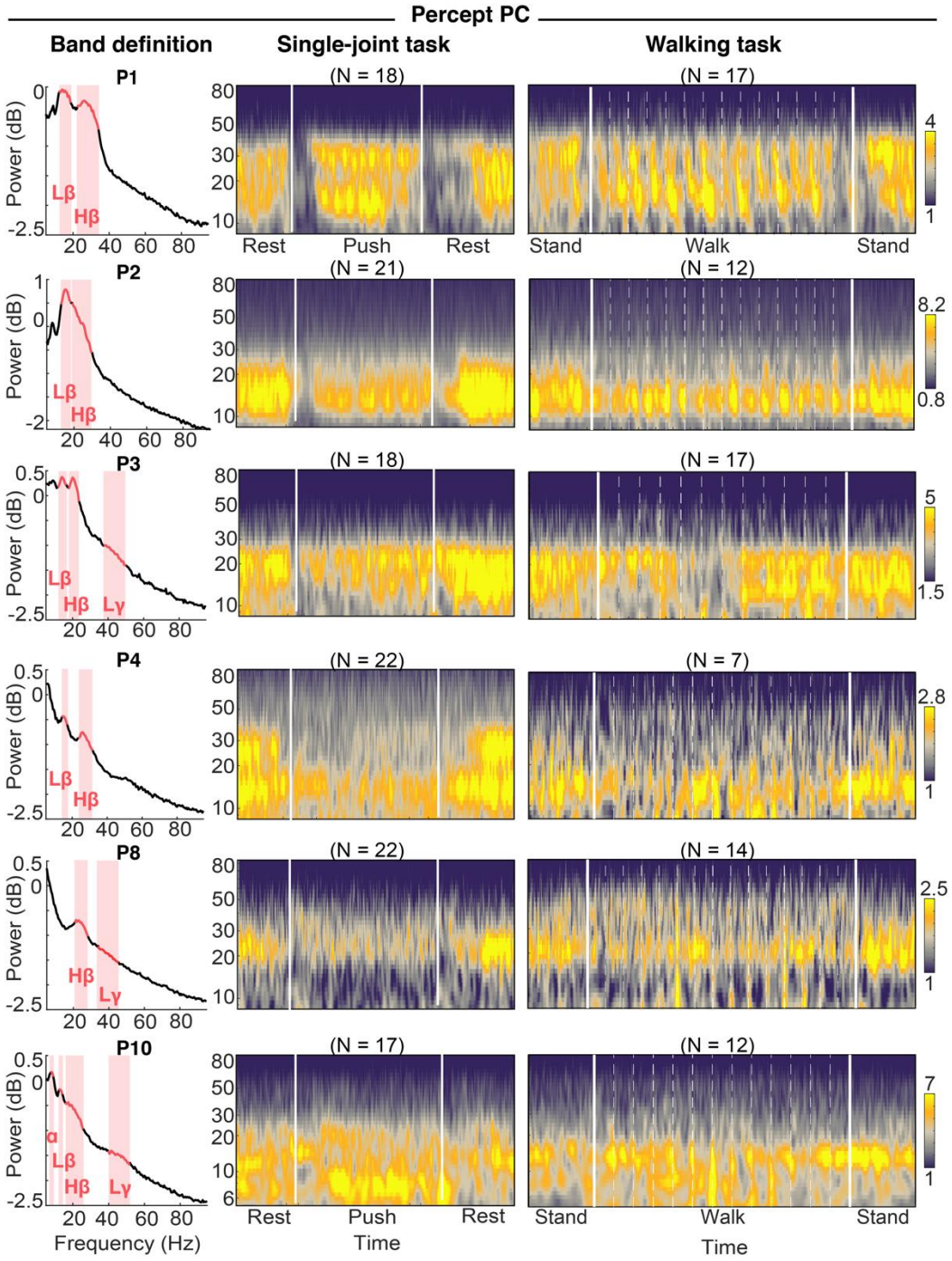

Fig. S5. Idiosyncratic encoding of leg muscle activation across tasks for patients implanted with a Percept PC stimulator. Left column: Power spectral densities highlight individual frequency bands across patients, as identified using an unbiased fitting algorithm (27). Middle column: Average (not normalized) scalograms during an isometric knee extension task in the neurorobotic platform. Vertical lines indicate the start and release of muscle contraction. Right column: Average scalograms (not normalized) for the walking task. Vertical lines indicate the initiation and termination of walking. Dashed lines correspond to foot strike events. Lβ, low beta band; Hβ, high beta band, Lγ, low gamma band.

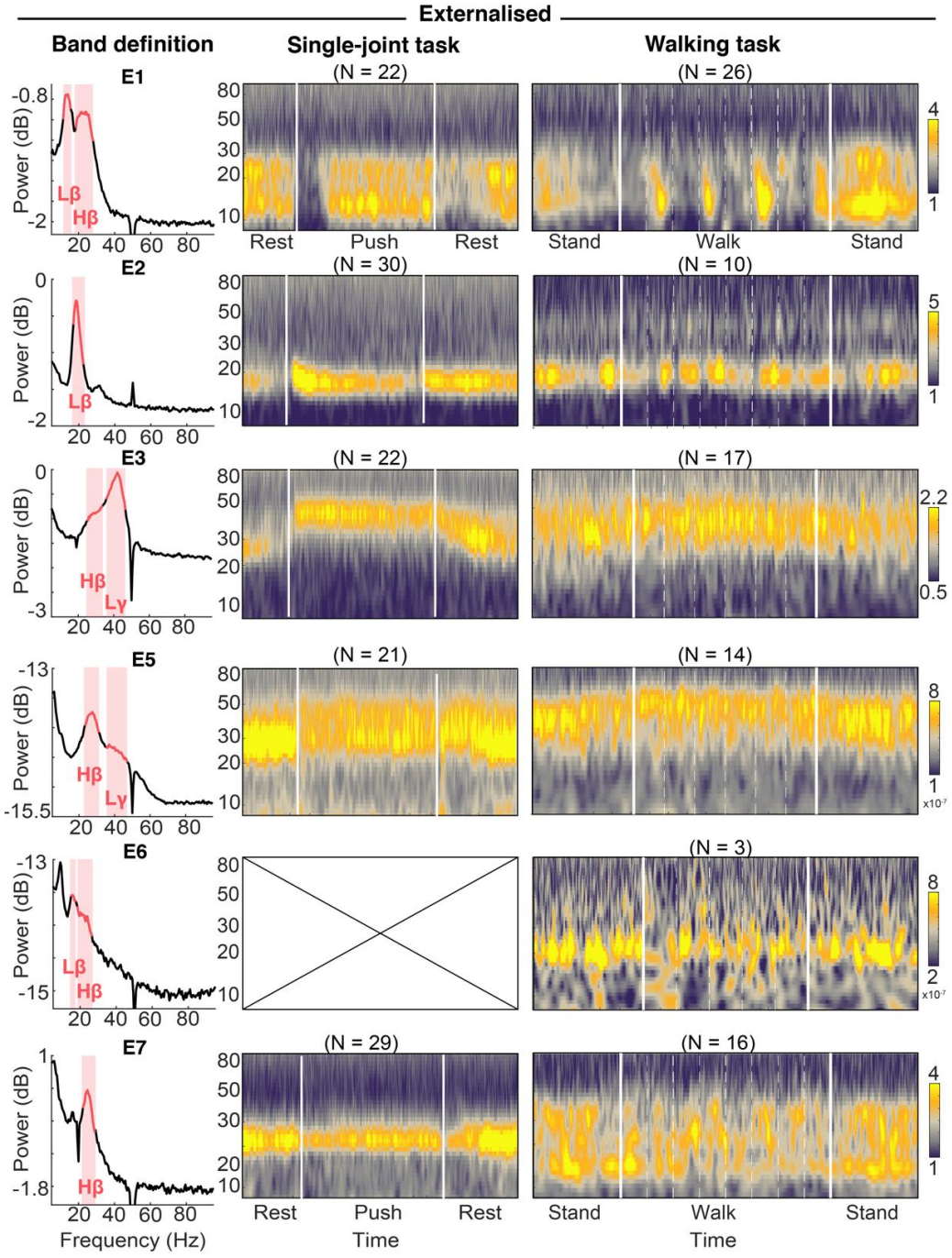

Fig. S6. Idiosyncratic encoding of leg muscle activation across tasks for patients recorded while their DBS leads externalized. Left column: Power spectral densities highlight individual frequency bands across patients. Middle column: Average (not normalized) scalograms during an isometric knee extension task in the neurorobotic platform. Vertical lines indicate the start and release of muscle contraction. Right column: Average scalograms (not normalized) for the walking task. Vertical lines indicate the initiation and termination of walking. Dashed lines correspond to foot strike events. Lβ, low beta band; Hβ, high beta band, Lγ, low gamma band.

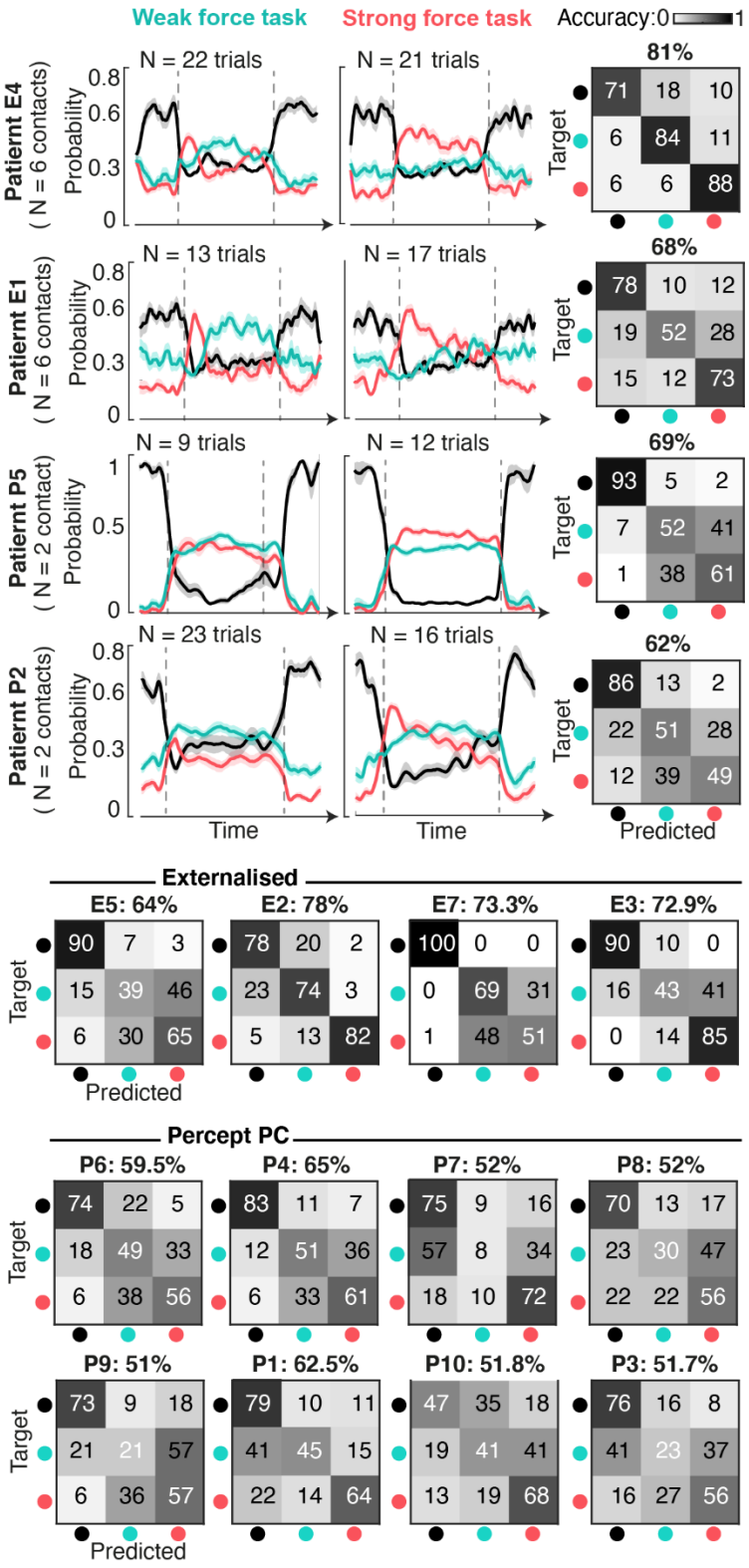

Fig. S7. Decoding performance of single-joint vigor tasks across patients. Temporal profiles of probability traces for four illustrative patients (two externalized E1 and E4, and two Percept P2 and P5), separately for weak and strong forces, along with sample-based confusion matrices across tasks of all the patients.

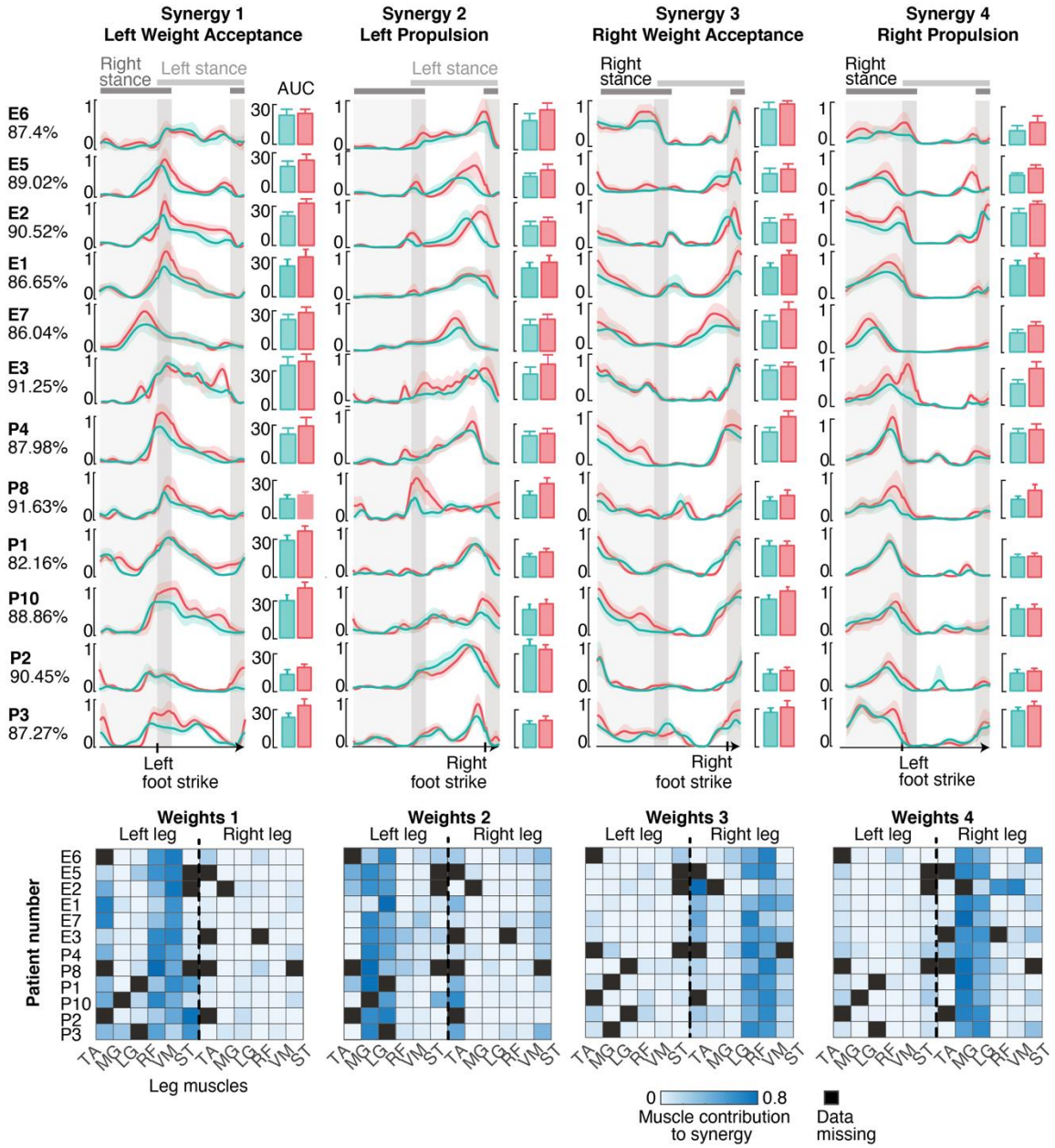

Fig. S8. Muscle synergies across patients. Temporal profiles of all extracted leg muscle synergies, percentage of variance explained and weights of muscle contribution for all the individual patients who performed the walking tasks.

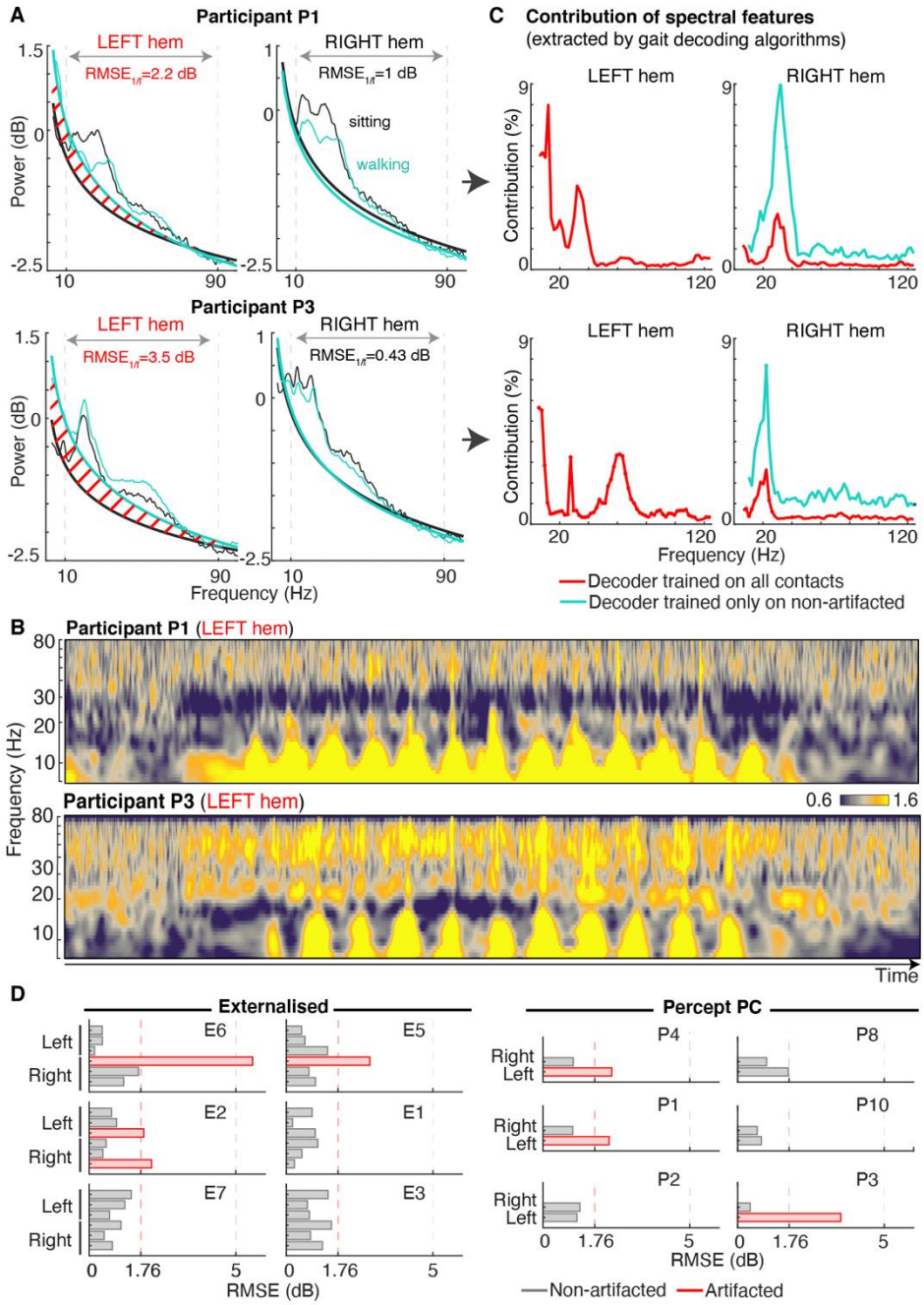

Fig. S9. Identification of artifacted channels during walking. For each contact pair, we compared the aperiodic (1/f) components of the PSD computed during sitting versus walking. Contacts that exhibited an increase in energy of 50% or more (1.76 dB) during walking in the range of interest (10-90Hz) were labeled as artifacted. (A) Illustrative example of bilateral PSD for two patients (P1 and P3), for whom one hemisphere was artifacted, and (B) spectrogram of the corrupted channels, showing gait-locked artifacts that emerge from low frequencies and propagate to high frequencies. (C) Comparison of the spectral features that contribute to the decoding algorithms when trained using all contacts (red) as compared to only using non-artifacted contacts (teal). Artifacted channels (Left hemisphere for P1 and P3) systematically exhibit predominant contributions of very low frequencies. Their removal does not significantly change the frequencies contributing from other channels. (D) Identification of artifacted channels for all contacts and patients.

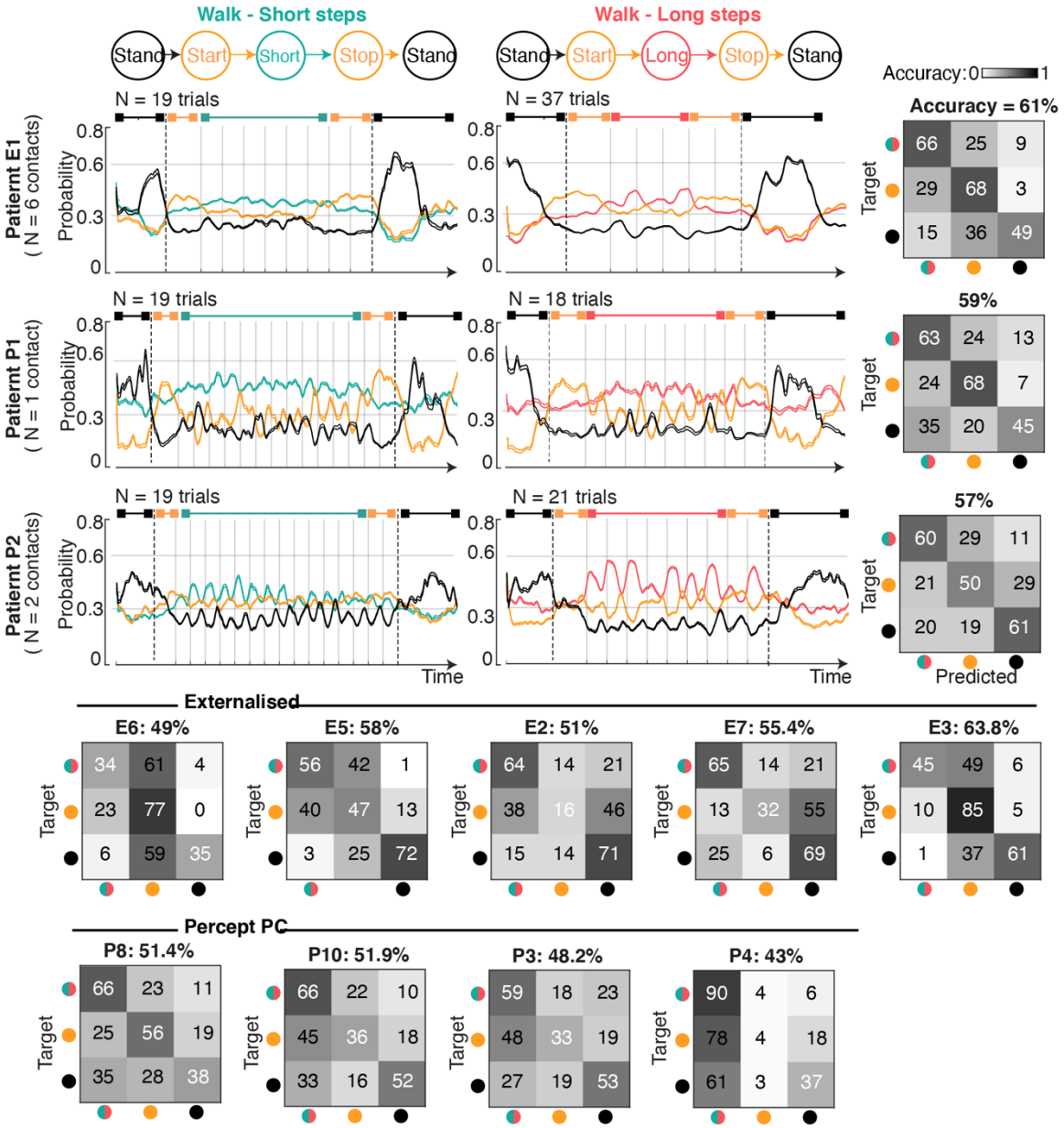

Fig. S10. Decoder of walking states across patients. Temporal profiles of probability traces for three patients (one externalized E1 and two Percept P1 and P2), separately for short and long steps, and sample-based confusion matrices of all patients.

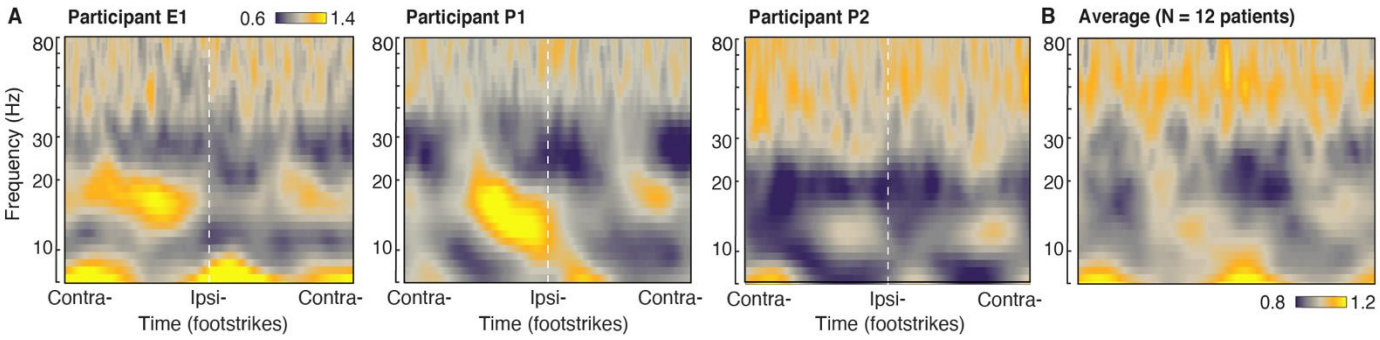

Fig. S11. STN LFP modulations per gait-cycle. (A) Illustrative examples of gait-cycle averaged spectrograms for three patients (one externalized E1 and two Percept P1 and P2), highlighting similar temporal patterns yet idiosyncratic frequency bands and modulation amplitudes. (B) Cross-patient average (N = 12).

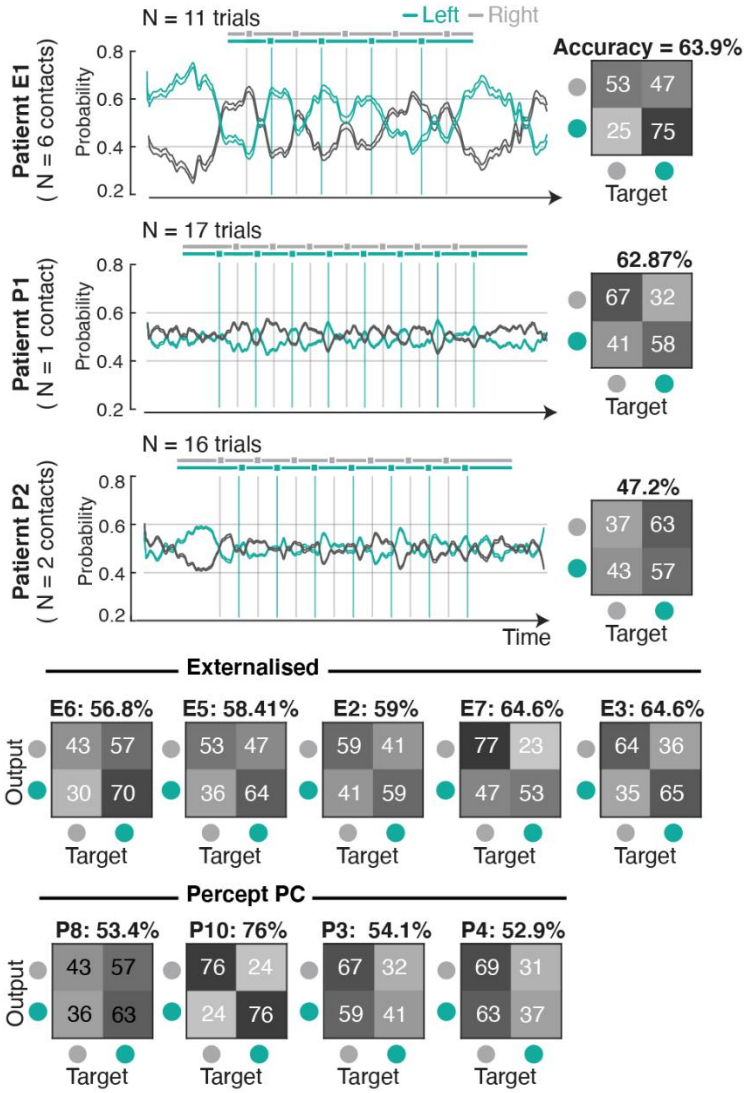

Fig. S12. Decoder of gait events across patients. Temporal profiles of probability traces for three patients (same as in fig. S11), along with sample-based confusion matrices of all the patients.

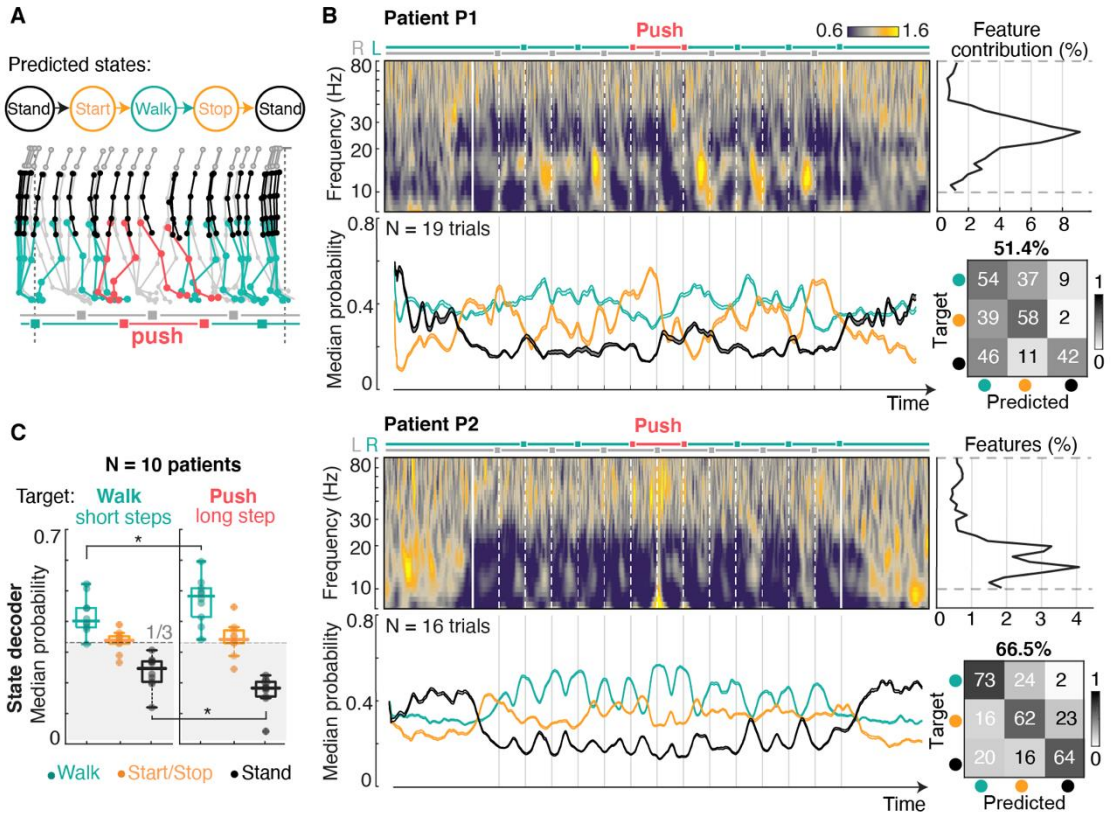

Fig. S13. Performance of walking-state decoder during gait adaptations. (A) We tested the walking-state decoder, trained on short and long steps, during a task requiring a sudden increase in effort during walking. (B) Illustrative examples of average spectrograms and probability traces for two patients. The step requiring a sudden increase in vigor (push) was either decoded as a transition (patient P1) due to the similarities to initiation and termination patterns, or with a higher probability of walking (patient P2). This depended on the amplitude of modulations in each individual patient. (C) Across all patients, the step with increased vigor translated into an increase of walking probabilities and a decrease of rest probabilities (* $p<0.05$).

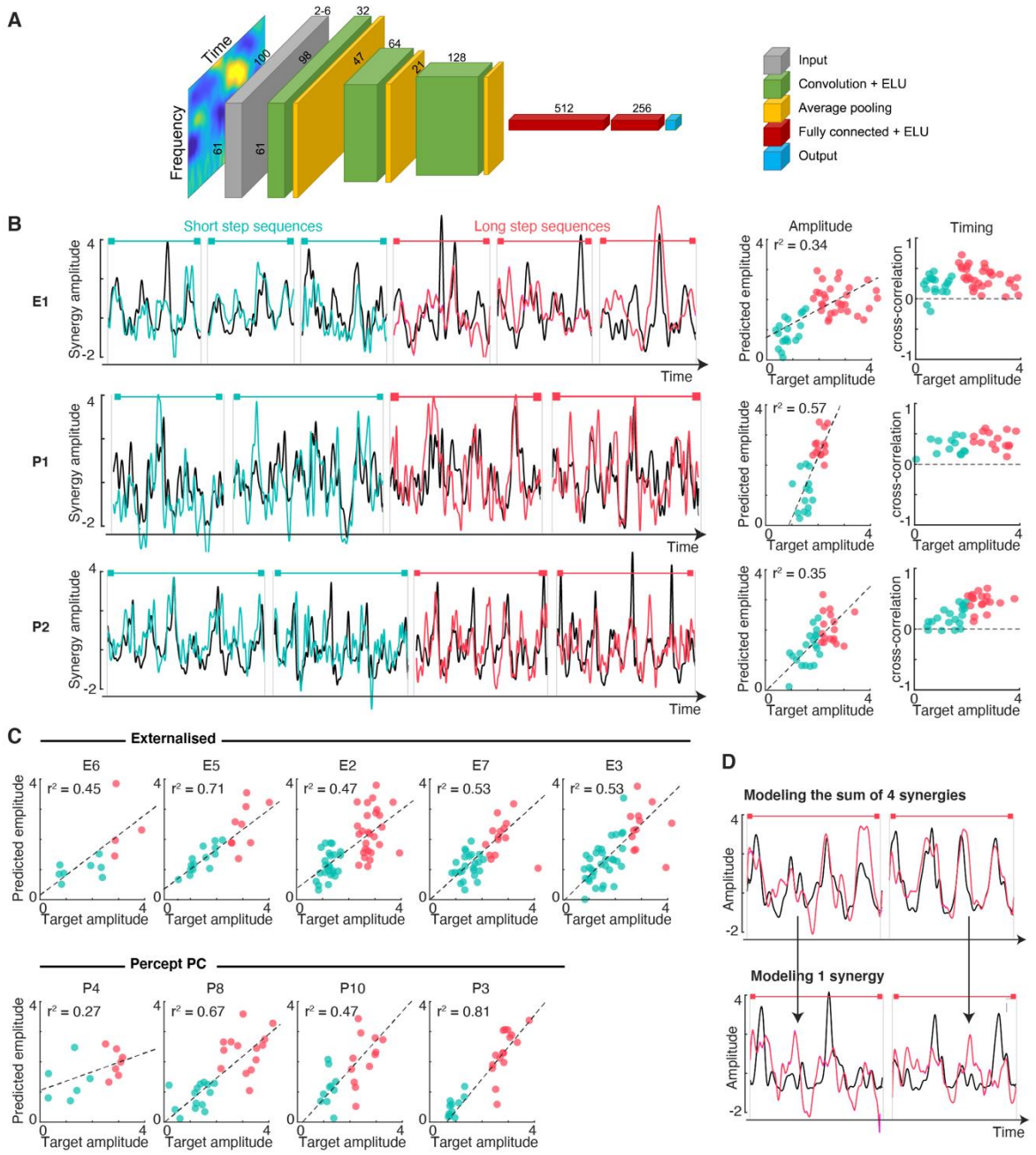

Fig. S14. Model of leg muscle synergy profiles using a deep learning algorithm across patients. (A) Structure of the deep neural network. (B) Comparison of target and modeled synergy traces for one externalized and two Percept PC patients, and (C) performance across patients. (D) Illustrative example of prediction output when modeling either all bilateral synergies (top) versus only one unilateral synergy (bottom). Using STN LFP, the deep learning model automatically predicted modulations happening twice per gait cycle, as expected from the bilateral encoding of leg movements in the STN.

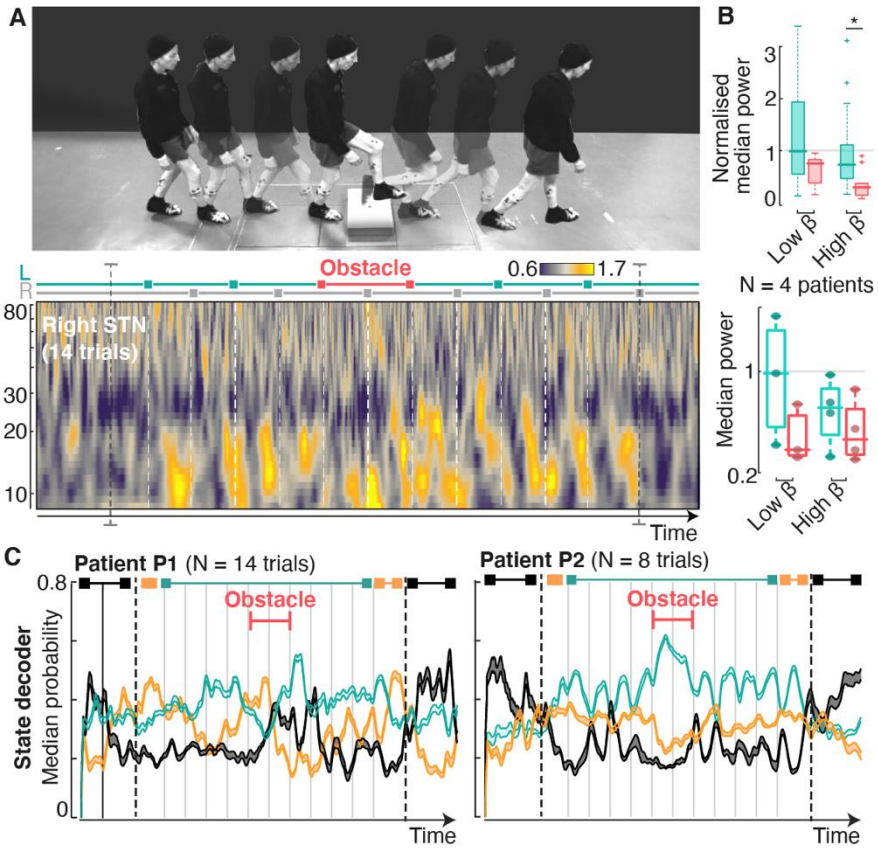

Fig. S15. STN LFP modulations during activities of daily living. (A) Time decomposition of a walking sequence (patient P1) that involves stepping over an obstacle. Chronophotography (top) and average spectrogram (bottom) highlight modulations in low and high beta that mirror the patterns observed during the horizontal ladder tasks. (B) Avoiding the obstacle induced modulations in low and high beta power (patient P1, top), as well across all tested patients (N=4, bottom). (C) Similar to what was observed during the sudden long step, the decoder (trained on short and long steps) predicted the obstacle as either a transition or with a bigger probability of walking (compared to rest).

SUPPLEMENTARY TABLES

ID	Sex	Age	Disease duration (years)	Dominant symptoms (AR or TD)	LED pre-op (mg eq.)	Total UPDRSIII (OFF/ON med, pre-Sx)	Most affected hemibody	Setup	Single-joint movement	Walk	Medication status
E4	M	60	12	AR+T	1437.5	27/14 (UPDRS)	Right	Externalized	X		OFF > 12h
E6	M	68	7	AR	1066,7	23/11 (UPDRS)		Externalized		X	OFF > 12h
										X	Residual
E5	M	52	13	AR	1453,3	25/12 (MDS-UPDRS)	Right	Externalized	X	X	Residual
E2	M	55	7	AR	700	30/7 (/142)	Right	Externalized	X	X	OFF > 12h
E1	M	70	6	AR+T	1087,5	43/23 (UPDRS)	Right	Externalized		X	OFF > 12h
									X	X	Residual
E7	M	65	15	AR	1600	35/14	Right	Externalized		X	Residual
E3	M	67	11	AR+T	1150	37/18 (MDS-UPDRS)	Left	Externalized	X	X	Residual
P6	M	71	8	AR	1670	31/9 (MDS-UPDRS)	Right	Percept	X	X	Residual
E8	F	43	5	AR+T	500	63/12 (/108)	Left	Externalized	X	X	ON
P4	M	60	7	AR+T	1350	45/33(1h)/18(2h) (MDS-UPDRS)	Right	Percept	X	X	ON
P5	M	72	13	AR	1600	30/9 (MDS-UPDRS)	Left	Percept	X		ON
									X		OFF > 12h
P7	M	57	7	AR+T	475	50/30 (MDS-UPDRS)	Right	Percept	X		ON
									X		Residual
P8	M	69	14	AR+T	1325	26/8	Right	Percept	X		OFF > 12h
P9	M	63	11	AR+T	1150	43/19 (MDS-UPDRS)	Right	Percept	X		OFF > 12h
									X	X	
P1	F	58	9	AR+T	1050	17/6 (MDS-UPDRS)	Right	Percept	X		OFF > 12h
										X	Residual
P10	M	52	17	T	1665	46/12 (MDS-UPDRS)	Right	Percept		X	
									X		Residual
P2	M	70	8	AR+T	1300	44/16	Right	Percept	X	X	OFF > 12h
P3	M	68	11	AR+T	1050	38/18 MDS-UPDRS	Left	Percept	X	X	ON

Table S1. Clinical details for all patients. Patients whose complete Parkinsonian medication was withdrawn 12h prior to experiments are indicated as “OFF>12h”. Patients who received some Levodopa medication within 3h before the experiment are labeled “ON”. Others (e.g., patients who retained some agonist medication, or those who received a delayed Levodopa dose the night before the experiment) are labeled as having some “residual” medication. LED: Levodopa equivalent dose.

SUPPLEMENTARY MOVIES

Movie S1. Neurorobotic platform to study the encoding of leg muscle activation in the STN.

This movie describes the modulations observed in STN LFP as patients performed various single-joint leg motor tasks while sitting in the neurorobotic platform, and the capacity to automatically decode force intensity from these signals in real-time.

Movie S2. Encoding of leg muscle activation in the STN

This movie describes the multimodal gait platform employed to record whole-body kinematics, bilateral leg muscle activity and STN LFP during unconstrained walking. The movie introduces the locomotor tasks performed, which interleaved short or long steps, and thus required weak or strong levels of muscle activation and force, as well as the LFP modulations associated with these movements.

Movie S3. Decoding of walking features from STN local field potentials

This movie introduces the results of decoding walking features directly from STN local field potentials. We show that our decoding platform allowed to decode (i) walking states, (ii) vigor, and (iii) dysfunctional aspects of walking such as freezing of gait.